Inorg. Chem. **2006**, *45*, 7252–7260

Bis(diisopropylphosphino)pyridine Iron Dicarbonyl, Dihydride, and Silyl Hydride Complexes

Ryan J. Trovitch, Emil Lobkovsky, and Paul J. Chirik*

Department of Chemistry and Chemical Biology, Baker Laboratory, Cornell University, Ithaca, New York 14853

Received May 18, 2006

Treatment of the bis(diisopropylphosphino)pyridine iron dichloride, (^{iPr}PNP)FeCl$_2$ (^{iPr}PNP = 2,6-(^{i}Pr$_2$PCH$_2$)$_2$(C$_5$H$_3$N)), with 2 equiv of NaBEt$_3$H under an atmosphere of dinitrogen furnished the diamagnetic iron(II) dihydride dinitrogen complex, (^{iPr}PNP)FeH$_2$(N$_2$). Addition of 1 equiv of PhSiH$_3$ to (^{iPr}PNP)FeH$_2$(N$_2$) resulted in exclusive substitution of the hydride trans to the pyridine to yield the silyl hydride dinitrogen compound, (^{iPr}PNP)FeH(SiH$_2$Ph)N$_2$, which has been characterized by X-ray diffraction. The solid-state structure established a distorted octahedral geometry where the hydride ligand distorts toward the iron silyl. Both (^{iPr}PNP)FeH$_2$(N$_2$) and (^{iPr}PNP)FeH(SiH$_2$Ph)N$_2$ form η^2-dihydrogen complexes upon exposure to H$_2$. The iron hydrides and the η^2-H$_2$ ligands are in rapid exchange in solution, consistent with the previously reported "cis" effect, arising from a dipole/induced dipole interaction between the two ligands. Taken together, the spectroscopic, structural, and reactivity studies highlight the relative electron-donating ability of this pincer ligand as compared to the redox-active aryl-substituted bis(imino)pyridines.

Introduction

Aryl-substituted bis(imino)pyridine iron complexes have emerged as a powerful class of catalysts for a host of important bond-forming reactions including olefin polymerization,[1] hydrogenation, and hydrosilation.[2] It is also now well-established that bis(imino)pyridines are both redox[3] and chemically active ligands,[4] participating in electron transfer, addition reactions, and deprotonation chemistry.[5,6] Recently, our laboratory has described the synthesis of the bis(imino)pyridine iron bis(dinitrogen) complex, (^{iPr}PDI)Fe(N$_2$)$_2$ (^{iPr}PDI = 2,6-(2,6-^{i}Pr$_2$−C$_6$H$_3$N═CMe)$_2$C$_5$H$_3$N) and its application to catalytic olefin and alkyne hydrogenation and hydrosilation reactions.[2] Investigations into the electronic structure of (^{iPr}PDI)Fe(N$_2$)$_2$ by Mössbauer spectroscopy and DFT calculations have established an intermediate-spin ferrous iron complexed by a bis(imino)pyridine dianion.[7] A similar electronic structure assignment has been suggested by Gambarotta and co-workers for the square planar bis(imino)pyridine iron methyl anion, [(^{iPr}PDI)FeMe]$^-$.[8]

While the electronic structure of (^{iPr}PDI)Fe(N$_2$)$_2$ has been elucidated, one open question is the role, if any, that the redox activity of the ligand plays in catalysis. Determining

* To whom correspondence should be addressed. E-mail: pc92@cornell.edu.

(1) (a) Ittel, S. D.; Johnson, L. K.; Brookhart, M. *Chem. Rev.* **2000**, *100*, 1169. (b) Small, B. L.; Brookhart, M.; Bennett, A. M. A. *J. Am. Chem. Soc.* **1998**, *120*, 4049. (c) Britovsek, G. J. P.; Gibson, V. C.; Kimberley, B. S.; Maddox, P. J.; McTavish, S. J.; Solan, G. A.; White, A. J. P.; Williams, D. J. *Chem. Commun.* **1998**, 849. (d) Britovsek, G. J. P.; Bruce, M.; Gibson, V. C.; Kimberley, B. S.; Maddox, P. J.; Mastroianni, S.; McTavish, S. J.; Redshaw, C.; Solan, G. A.; Strömberg, S.; White, A. J. P.; Williams, D. J. *J. Am. Chem. Soc.* **1999**, *121*, 8728. (e) Gibson, V. C.; Spitzmesser, S. K. *Chem. Rev.* **2003**, *103*, 283. (f) Bianchini, C.; Mantovani, G.; Meli, A.; Migliacci, D.; Zanobini, F.; Laschi, F.; Sommazzi, A. *Eur. J. Inorg. Chem.* **2003**, 1620. (f) Bouwkamp, M. W.; Lobkovsky, E.; Chirik, P. J. *J. Am. Chem. Soc.* **2005**, *127*, 9660.

(2) Bart, S. C.; Lobkovsky, E.; Chirik, P. J. *J. Am. Chem. Soc.* **2004**, *126*, 13794.

(3) (a) de Bruin, B.; Bill, E.; Bothe, E.; Weyhermüller, T.; Wieghardt, K. *Inorg. Chem.* **2000**, *39*, 2936. (b) Budzelaar, P. H. M.; de Bruin, B.; Gal, A. W.; Wieghardt, K.; van Lenthe, J. H. *Inorg. Chem.* **2001**, *40*, 4649. (c) Sugiyama, I.; Korobkov, I.; Gambarotta, S.; Mueller, A.; Budzelaar, P. H. M. *Inorg. Chem.* **2004**, *43*, 5771. (d) Scott, J.; Gambarotta, S.; Korobkov, I.; Knijnenburg, Q.; de Bruin, B.; Budzelaar, P. H. M. *J. Am. Chem. Soc.* **2005**, *127*, 17204.

(4) For examples see: (a) Clentsmith, G. K. B.; Gibson, V. C.; Hitchcock, P. B.; Kimberely, B. S.; Rees, C. W. *Chem. Commun.* **2002**, 1498. (b) Korobkov, I.; Gambarotta, S.; Yap, G. P. A.; Budzelaar, P. H. M. *Organometallics* **2002**, *21*, 3088. (c) Kooistra, T. M.; Hetterscheid, D. G. H.; Schwartz, E.; Knijnenburg, Q.; Budzelaar, P. H. M.; Gal, A. W. *Inorg. Chim. Acta* **2004**, *357*, 2945. (d) Blackmore, I. J.; Gibson, V. C.; Hitchcock, P. B.; Rees, C. W.; Williams, D. J.; White, A. J. P. *J. Am. Chem. Soc.* **2005**, *127*, 6012.

(5) Bouwkamp, M. W.; Lobkovsky, E.; Chirik, P. J. *Inorg. Chem.* **2006**, *45*, 2.

(6) Reardon, D.; Aharonian, G.; Gambarotta, S.; Yap, G. P. A.; Budzelaar, P. H. M. *J. Am. Chem. Soc.* **2002**, *124*, 12268.

(7) Bart, S. C.; Chlopek, K.; Bill, E.; Bouwkamp, M. W.; Lobkovsky, E.; Neese, F.; Weighardt, K.; Chirik, P. J. submitted.

(8) Scott, J.; Gambarotta, S.; Korobkov, I.; Budzelaar, P. H. M. *Organometallics* **2005**, *24*, 6298.

10.1021/ic0608647 CCC: $33.50
Published on Web 08/05/2006

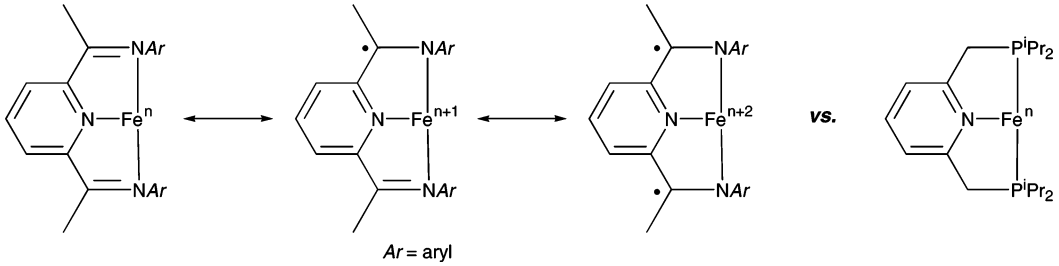

Figure 1. Comparison of redox-active bis(imino)pyridine to bis(phosphino)pyridine pincer ligands.

the answer to such a question is extremely challenging, as many factors are often responsible for catalyst (in)activity. Efforts are now underway in our laboratory aimed at experimentally evaluating whether metal−ligand electron transfer events are a prerequisite for catalytically active iron centers and how these properties can be tuned for optimal performance. To this end, we sought to modify the bis(imino)pyridine ligand core by replacing the unsaturated imine donors with saturated dialkylphosphines (Figure 1), thereby disrupting the conjugated π-system and increasing the barrier for metal−ligand redox events.[9] In this contribution, we report the synthesis, characterization, and evaluation of the catalytic activity of bis(phosphino)pyridine iron complexes and compare the structures, electronic properties, and reactivity to established bis(imino)pyridine compounds.

Results and Discussion

Synthesis of Bis(diisopropylphosphino)pyridine Iron Dicarbonyl, Dihydride, and Silyl Hydride Compounds. To gain insight into the relative electronic environments imparted by the bis(phosphine) versus bis(imine) ligands, the dicarbonyl complex, (^{iPr}PNP)Fe(CO)$_2$ **(1-(CO)$_2$)** was targeted. Milstein and co-workers have recently reported the synthesis of (^{iPr}PNP)FeCl$_2$ **(1-Cl$_2$)** by straightforward complexation of the free ligand[10] with ferrous dichloride.[11] Stirring **1-Cl$_2$** with an excess of 0.5% sodium amalgam in the presence of 4 atm of carbon monoxide furnished a red solid identified as **1-(CO)$_2$**, based on NMR and IR spectroscopies, combustion analysis, and single-crystal X-ray diffraction (eq 1).

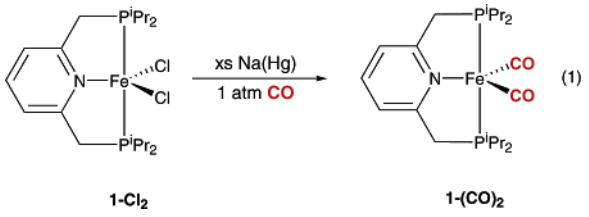

In the solid-state (KBr) infrared spectrum, two intense carbonyl bands were observed at 1842 and 1794 cm^{-1}, substantially reduced from the peaks reported at 1950 and 1894 cm^{-1} for (^{iPr}PDI)Fe(CO)$_2$ in the same medium. The dramatic shift of the CO bands to lower frequencies is consistent with a more reducing iron(0) center in **1-(CO)$_2$** as compared to the more oxidized iron in (^{iPr}PDI)Fe(CO)$_2$.

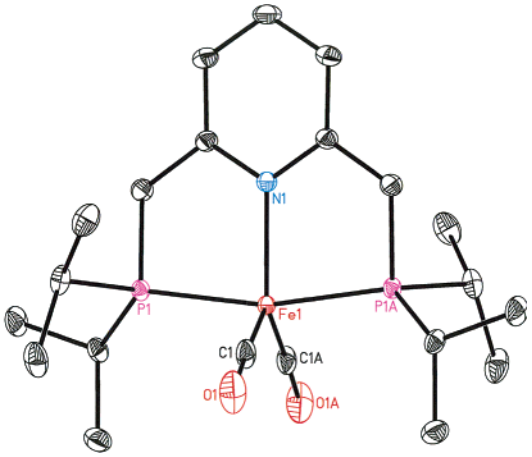

Figure 2. Molecular structure of **1-(CO)$_2$** depicted with 30% probability ellipsoids. Hydrogen atoms omitted for clarity.

Table 1. Selected Bond Distances (Å) and Angles (deg) for **1-(CO)$_2$**

	1-(CO)$_2$	**(^{i}PrPDI)Fe(CO)$_2$**
Fe(1)−C(1)	1.7325(9)	1.7809(19) (apical)
Fe(1)−C(1A)	1.7325(9)	1.7823(19) (basal)
Fe(1)−P(1)	2.1941(2)	−
Fe(1)−N(1)	2.0684(8)	1.8488(14)
C(1)−O(1)	1.1734(11)	1.147(2)
N(1)−C(3)	1.3593(9)	1.376(2)
P(1)−Fe(1)−P(1A)	165.990(12)	−
C(1)−Fe(1)−C(1A)	119.91(7)	97.01(9)
N(1)−Fe(1)−P(1)	82.995(6)	−
C(1)−Fe(1)−N(1)	120.04(3)	157.89(8)

Cooling a concentrated toluene solution of **1-(CO)$_2$** to −35 °C produced single crystals suitable for X-ray diffraction. The solid-state structure is presented in Figure 2, and selected metrical parameters are reported in Table 1. The overall geometry about the iron in **1-(CO)$_2$** is best described as idealized trigonal bipyramidal, in contrast to the distorted square pyramidal structure observed for (^{iPr}PDI)Fe(CO)$_2$. In **1-(CO)$_2$**, the two carbonyl ligands and the pyridine nitrogen define the equatorial plane with bond angles of 119.91(7)° and 120.04(3)° for C(1)−Fe(1)−C(1A) and C(1)−Fe(1)−N(1), respectively. The carbonyls and the phosphine substituents are related by symmetry. The pyridine ring is slightly canted with respect to the iron−bis(phosphine) plane. The only significant distortion observed is in the axial phosphine ligands where the P(1)−Fe(1)−P(1A) bond angle of 165.990(12)° is contracted toward the pyridine ring. The bis(imino)pyridine iron dicarbonyl, (^{iPr}PDI)Fe(CO)$_2$, has a more contracted C−Fe−C angle of 97.01(9)° between the

(9) For a recent example of a singly reduced pincer ligand, see: Frech, C. M.; Ben-David, Y.; Weiner, L.; Milstein, D. *J. Am. Chem. Soc.* **2006**, *128*, 7128.
(10) Jansen, A.; Pitter, S. *Montasch. Chem.* **1999**, *130*, 783.
(11) Zhang, J.; Gandelman, M.; Herrman, D.; Leitus, G.; Shimon, L. J. W.; Ben-David, Y.; Milstein, D. *Inorg. Chim. Acta* **2006**, *359*, 1955.

carbonyl ligands, consistent with a square pyramidal geometry and reduced π-back-bonding.

The more reducing iron center in **1-(CO)$_2$** as compared to (^{iPr}PDI)Fe(CO)$_2$ is also evident in the bond distances of the carbonyl ligands. In the phosphine-substituted compound, **1-(CO)$_2$**, contracted Fe−C bond distances of 1.7325(9) Å are observed along with elongated C−O bond lengths of 1.1734(11) Å. By way of comparison, the corresponding distances in (^{iPr}PDI)Fe(CO)$_2$ are 1.7809(19)/1.7823(19) and 1.147(2) Å, respectively, consistent with a more oxidized iron center. Another interesting comparison are the structural features of **1-(CO)$_2$** and the corresponding ferrous dihalide. For the latter class of compound, the only structurally characterized example is the bis(*tert*-butyl)-substituted derivative, (^{tBu}PNP)FeCl$_2$.[11] The molecular geometry of the dichloride compound is best described as distorted square pyramidal with the iron atom raised out of the idealized basal plane by 0.552 Å. Accordingly, the iron−pyridine bond distance is elongated to 2.303(2) Å, as compared 2.0684(8) Å in **1-(CO)$_2$**.

Attempts to synthesize a bis(phosphino)pyridine iron dinitrogen complex analogous to (^{iPr}PDI)Fe(N$_2$)$_2$[2] have been unsuccessful. Stirring a pentane or toluene solution of **1-Cl$_2$** or **1-Br$_2$** with excess 0.5% sodium amalgam under N$_2$ resulted in an intractable mixture of iron products and free ^{iPr}PNP ligand. An alternative route to (^{iPr}PDI)Fe(N$_2$)$_2$ involves treatment of (^{iPr}PDI)FeBr$_2$ with 2 equiv of NaBEt$_3$H under a dinitrogen atmosphere. Presumably, the transient iron dihydride undergoes reductive elimination of H$_2$ and the reduced iron fragment captures dinitrogen to furnish the observed product. Treatment of a thawing ethereal slurry of **1-Cl$_2$** with 2 equiv of NaBEt$_3$H under an atmosphere of dinitrogen resulted in isolation of a diamagnetic, red-orange solid identified as (^{iPr}PNP)FeH$_2$(N$_2$) **(1-H$_2$(N$_2$))** (eq 2).

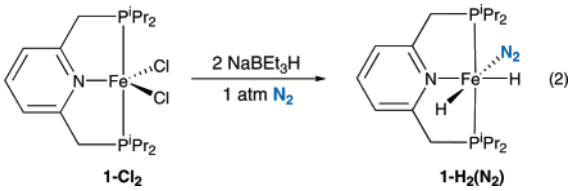

Unfortunately, **1-H$_2$(N$_2$)** has proven extremely difficult to handle, undergoing decomposition to free ^{iPr}PNP and insoluble iron products over the course of hours in benzene-d_6 solution at 23 °C. This unwanted side reaction complicates characterization by ^{1}H NMR spectroscopy, as small amounts of decomposition (~5−10%) significantly broaden spectra to where peaks for **1-H$_2$(N$_2$)** cannot be readily identified.

Collecting data immediately following purification allowed characterization of **1-H$_2$(N$_2$)** by multinuclear NMR spectroscopy. In benzene-d_6, the ^{1}H NMR spectrum exhibited the number of resonances expected for an idealized C_s-symmetric molecule with the mirror plane containing the two hydrides and the dinitrogen ligand. Two triplets of doublets centered at −17.65 and −12.54 ppm were observed, diagnostic of inequivalent iron−hydride resonances. The appearance of two inequivalent iron hydrides eliminates the C_{2v}-symmetric isomer where the Fe−H ligands are in a trans arrangement. This isomer is also disfavored due to the strong trans influence of the hydride ligand.[12] In addition, a single ^{31}P resonance peak was observed at 108.28 ppm for the equivalent phosphines. Coordination of the dinitrogen ligand was confirmed by solid-state (KBr) infrared spectroscopy with the observation of a strong N≡N band centered at 2016 cm^{-1}. This value is reduced compared to the corresponding N$_2$ stretching frequencies of 2124 and 2053 cm^{-1} reported for (^{iPr}PDI)Fe(N$_2$)$_2$, again highlighting a more reducing iron center engendered by the ^{iPr}PNP ligand.

Assignment of **1-H$_2$(N$_2$)** as an iron(II) dihydride rather than an iron(0) dihydrogen complex is supported by T_1(min) measurements and the phosphorus−iron−hydride coupling constant. A T_1(min) value of 314 ms was measured at −25 °C in toluene-d_8 at 500 MHz and in combination with the $^2J_{P-H}$ values of 52 and 60.5 Hz is consistent with the ferrous dihydride formulation.[13,14] While the iron-hydride peaks appear as a sharp triplet of doublets at 23 °C, one-dimensional EXSY NMR experiments indicate rapid exchange between the iron-hydride positions, demonstrating that reductive coupling to form an iron(0) η^2-dihydrogen complex, followed by rapid η^2-H$_2$ rotation[15] or N$_2$ dissociation to form the five-coordinate iron(II) dihydride, is competitive on the NMR time scale. This observation, along with the H−H coupling constant of 21.5 Hz, suggest some "stretched η^2-dihydrogen" character.[16]

The formation of the iron(II) dihydride is interesting in light of the observations with the corresponding bis(imino)pyridine compound. Treatment of (^{iPr}PDI)FeCl$_2$ with NaBEt$_3$H in the presence of N$_2$ resulted in isolation of the bis(dinitrogen) complex, (^{iPr}PDI)Fe(N$_2$)$_2$, presumably from rapid reductive coupling of the two iron hydrides followed by dissociation. Consistent with this hypothesis is the formation of the iron dihydrogen complex, (^{iPr}PDI)Fe(η^2-H$_2$), upon exposure of (^{iPr}PDI)Fe(N$_2$)$_2$ to 1 atm of H$_2$. The instability of (^{iPr}PDI)Fe(η^2-H$_2$) was further demonstrated by the observation of rapid reversion to (^{iPr}PDI)Fe(N$_2$)$_2$ upon exposure to even trace amounts of dinitrogen. The relative stability of the oxidative addition products, **1-H$_2$(N$_2$)** versus the putative "(^{iPr}PDI)FeH$_2$" is a consequence of the relative donor abilities of the ligand and hence the reducing nature of the iron center.[2] In the ^{iPr}PNP case, the more electron donating, redox innocent ligand engenders a more electron rich metal center and stabilizes the iron(II) dihydride. In the bis(imino)pyridine compound, the "redox activity" of the ligand, generating an [^{iPr}PDI]$^{2-}$ chelate produces a more oxidizing iron center where the requisite two electrons for H$_2$ oxidative addition are stored in the bis(imino)pyridine π-system. It is also important to note that the redox properties of the two

(12) Jordan, R. B. In *Reaction Mechanisms of Inorganic and Organometallic Systems*, 2nd ed.; Oxford University Press: New York, 1998; pp 64−67.
(13) Desrosiers, P. J.; Cai, L.; Lin, Z.; Richards, R.; Halpern, J. *J. Am. Chem. Soc.* **1991**, *113*, 4173.
(14) Kubas, G. J. *Acc. Chem. Res.* **1988**, *21*, 120.
(15) For studies describing the low rotational barriers of η^2-H$_2$ ligands, see: Eckert, J.; Kubas, G. J. *J. Phys. Chem.* **1993**, *97*, 2378.
(16) Heinekey, D. M.; Lledos, A.; Lluch, J. M. *Chem. Soc. Rev.* **2004**, *33*, 175.

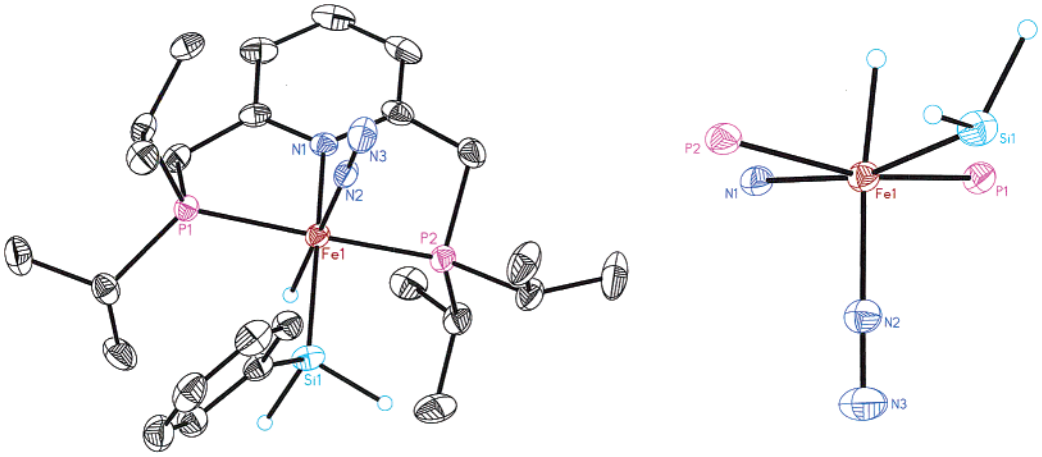

Figure 3. Molecular structure of the core of **1-H(Si)N$_2$** depicted with 30% probability ellipsoids (left) and a view of the core of the molecule (right). Hydrogen atoms, except for the iron-hydride and silicon hydrogens, omitted for clarity.

compounds are also attenuated by the ligand substituents. The bis(imino)pyridine ligand contains relatively electron-poor aryl groups, while the phosphines are substituted with electron-donating alkyl substituents. Attempts to prepare the corresponding iron compound bearing aryl-substituted PNP ligands are currently under investigation in our laboratory.

Treatment of **1-H$_2$(N$_2$)** with 1 equiv of $PhSiH_3$ resulted in replacement of one of the hydride ligands for the silyl to yield solely one isomer of **1-H(Si)N$_2$** (eq 3). This molecule

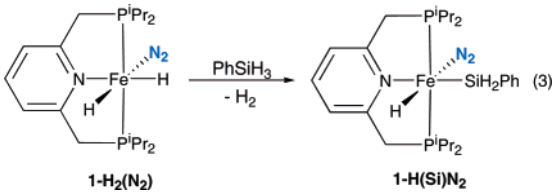

was also conveniently prepared by treatment of **1-Cl$_2$** with 2 equiv of $NaBEt_3H$ in the presence of a stoichiometric quantity of $PhSiH_3$. A single iron hydride resonance was observed at −13.12 ppm as a triplet ($^2J_{P-H}$ = 58 Hz) in the benzene-d_6 ^{1}H NMR spectrum, arising from coupling to two equivalent phosphine ligands. The ^{31}P NMR spectrum exhibited a single peak at 96.85 ppm, shifted upfield from the value observed for **1-H$_2$(N$_2$)**. Diastereotopic Si−*H* resonances were observed by ^{1}H NMR spectroscopy as overlapping triplets centered at 4.94 ppm with $^3J_{P-H}$ = 5.5 Hz. EXSY NMR spectroscopy (500 ms mixing time) demonstrated that the iron-hydride and the silicon hydrogens do not undergo exchange on the NMR time scale at 23 °C. Moreover, the iron-hydride resonance has a T_1(min) value of 368 ms at −50 °C at 500 MHz. Taken together, these data suggest that reductive coupling to form an iron−silane σ-complex followed by rotation and oxidative addition has a higher barrier than that associated process with the corresponding η^2-dihydrogen compound. These results again highlight the electron-donating ability of the ^{iPr}PNP ligand as compared to the bis(imino)pyridine where a bis(η^2-silane) complex has been crystallographically characterized.[2]

The presence of a coordinated dinitrogen ligand was confirmed by solid-state (KBr) infrared spectroscopy with the observation of a strong band centered at 2032 cm^{-1}, a value shifted to a significantly higher frequency than the N_2 stretch observed in **1-H$_2$(N$_2$)** (ν_{NN} = 2016 cm^{-1}), demonstrating a more electropositive iron center upon replacing hydride with silyl. Importantly, **1-H(Si)N$_2$** was stable in ambient temperature benzene-d_6 solutions indefinitely, allowing further characterization and reactivity studies.

Table 2. Selected Bond Distances (Å) and Angles (deg) for **1-H(Si)N$_2$** and **1-H(Si)CO**

	1-H(Si)N$_2$	**1-H(Si)CO**
Fe(1)−H(1M)	1.512(19)	1.522(15)
Fe(1)−P(1)	2.1823(5)	2.1780(5)
Fe(1)−P(2)	2.1817(5)	2.1827(4)
Fe(1)−N(1)	2.0370(15)	2.0605(13)
Fe(1)−Si(1)	2.2718(6)	2.2689(5)
Fe(1)−N(2)/C(26)	1.8002(17)	1.7541(16)
N(2)−N(3)/C(26)−O(1)	1.120(2)	1.1635(19)
Si(1)−H(1M)	2.420(17)	2.41(2)
N(1)−C(2)	1.362(2)	1.359(2)
P(1)−Fe(1)−P(2)	161.12(2)	160.761(19)
N(1)−Fe(1)−Si(1)	165.90(4)	167.02(4)
H(1M)−Fe(1)−N(2)/C(26)	173.3(7)	166.2(9)
N(1)−Fe(1)−N(2)/C(26)	96.82(6)	102.36(6)
Si(1)−Fe(1)−N(2)/C(26)	97.04(5)	90.46(5)
H(1M)−Fe(1)−P(1)	80.6(7)	81.8(9)
H(1M)−Fe(1)−P(2)	86.6(7)	85.6(9)
H(1M)−Fe(1)−Si(1)	76.6(7)	75.9(9)

The solid-state structure of **1-H(Si)N$_2$** was determined by single-crystal X-ray diffraction (Figure 3) and definitively established the trans arrangement of the silyl and pyridine nitrogen and the dinitrogen and iron-hydride, respectively. The data were of sufficient quality such that all of the hydrogens were located and refined. The metrical parameters (Table 2) reveal an overall molecular geometry distorted from idealized octahedral. The chelate-constrained P(1)−Fe(1)−P(2) angle is 161.12(2)° and is also bent away from the π-acidic dinitrogen ligand with H(1M)−Fe(1)−P(1) and H(1M)−Fe(1)−P(2) angles of 80.6(7)° and 86.6(7)°, respectively. Similar distortions have been observed in bis(diphosphino) iron hydride, dihydrogen cations, and *trans*-[(P−P)$_2$Fe(H)(η^2-H$_2$)]$^+$ (P−P = chelating bis(phosphine)) and are believed to hybridize the metal orbitals to increase back-bonding to the π-acid.[17] The iron hydride is also

(17) Maseras, F.; Duran, M.; Lledõs, A.; Bertrán, J. *J. Am. Chem. Soc.* **1991**, *113*, 2879.

directed toward the silyl ligand with an H(1M)−Fe(1)−Si(1) bond angle of 76.6(7)°, suggestive of a weak interaction. However, the distance between the iron-hydride and silicon atom is 2.420(17) Å, well outside the sum of the covalent radii for a silicon−hydrogen bond.

The iron−phosphorus bond distances (Table 2) of 2.1823(5) and 2.1817(5) Å are comparable to those found in **1-(CO)$_2$**, and the N(2)−N(3) distance of 1.120(2) Å is as expected for a weakly activated dinitrogen ligand. The Fe(1)−H(1M) distance of 1.512(19) Å is in agreement with iron-hydrides characterized by neutron diffraction.[18−20] The carbon−nitrogen pyridine distance, N(1)−C(2), of 1.362(2) Å is contracted as compared to the values of 1.37−1.39 Å typically found in reduced bis(imino)pyridine ligands, demonstrating that ^{iPr}PNP acts as a σ-donor ligand and is not engaged in redox processes with the iron.

Evaluation of Catalytic Activity and Ligand Substitution Reactions. With the ferrous dihydride, **1-H$_2$(N$_2$)**, and silyl hydride, **1-H(Si)N$_2$**, in hand, the catalytic activity of both compounds was assayed. The hydrogenation and hydrosilation of simple, unactivated olefins such as 1-hexene and cyclohexene were chosen as model reactions to compare to the catalytic activity to the bis(imino)pyridine iron catalyst precursor, (^{iPr}PDI)Fe(N$_2$)$_2$.[2] Hydrogenation of 1-hexene with 0.3 mol % of **1-H$_2$(N$_2$)** and 4 atm of H$_2$ in pentane solution was complete (>98% conversion, GC) after stirring for 3 h at 23 °C, substantially longer than the few minutes required with (^{iPr}PDI)Fe(N$_2$)$_2$. Attempts to hydrogenate cyclohexene with **1-H$_2$(N$_2$)** under identical conditions produced only minimal conversion (~10%) after 6 and 24 h, owing to catalyst decomposition over the course of the reaction. The ferrous silyl hydride, **1-H(Si)N$_2$**, was not effective for the hydrosilation of 1-hexene or cyclohexene with PhSiH$_3$.

The origin of the poor catalytic performance was studied in more detail by evaluation of a series of stoichiometric processes. Exposure of **1-H$_2$(N$_2$)** to 4 atm of dihydrogen resulted in gradual disappearance of the starting material with concomitant growth of a new product over the course of 3 h at 23 °C. Importantly, iron hydride resonances for both compounds were observed simultaneously. The product exhibited a broad iron-hydride signal ($\Delta\nu_{1/2}$ = 12 Hz) centered at −11.17 ppm. Cooling the sample to −75 °C resulted in gradual broadening of the peak ($\Delta\nu_{1/2}$ = 46 Hz, −75 °C) without resolution. On the basis of this observation and results described below, we tentatively assign the product as the iron hydride dihydrogen complex, **1-H$_2$(H$_2$)**. Definitive characterization of this compound was again hampered by competing decomposition processes involving loss of the pincer ligand and formation of insoluble iron species. However, the observation of a newly formed, single, broad iron hydride resonance suggests that the N$_2$ ligand undergoes

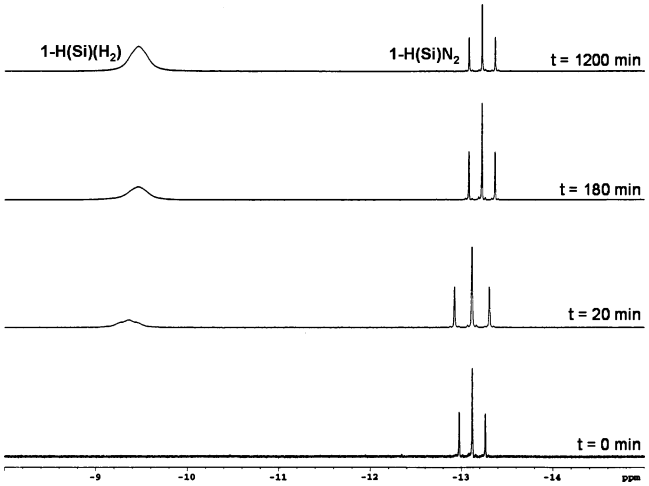

Figure 4. Hydride region of the ^{1}H NMR spectrum of the hydrogenation of **1-H(Si)N$_2$** as a function of time.

dissociation followed by coordination of a molecule of dihydrogen that is in rapid exchange with the iron hydride (eq 4).

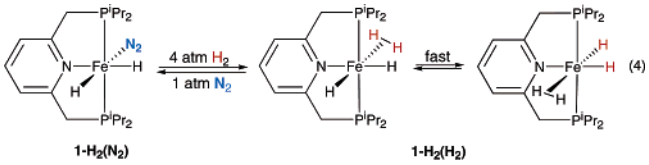

On the basis of the limited experimental data available, we are unable to definitively assign the isomers of **1-H$_2$(H$_2$)**. In addition to those depicted in eq 4, the isomer where the dihydrogen ligand is trans to the pyridine nitrogen is also possible but is most likely disfavored due to the strong trans influence of the hydride ligands. Treatment of **1-H$_2$(N$_2$)** with D$_2$ gas resulted in rapid isotopic exchange with the iron hydride positions. In related experiments, exposure of either **1-H$_2$(H$_2$)** or **1-D$_2$(D$_2$)** to 1 atm of dinitrogen resulted in displacement of the η^2-dihydrogen or dideuterium ligand to rapidly regenerate **1-H$_2$(N$_2$)** or **1-D$_2$(D$_2$)**. Notably, the reversion to **1-H$_2$(N$_2$)** with 1 atm of N$_2$ is faster than formation of **1-H$_2$(H$_2$)** with 4 atm of dihydrogen, demonstrating N$_2$ is a better ligand than H$_2$.

The greater solution stability of **1-H(Si)N$_2$**, relative to **1-H$_2$(N$_2$)**, suggested that the corresponding dihydrogen complexes could also be longer lived and allow more thorough characterization. Addition of 4 atm of H$_2$ to **1-H(Si)N$_2$** resulted in gradual disappearance of the iron hydride signal centered at −13.12 ppm with concomitant growth of a new, broad signal at −9.37 ppm (Figure 4). This new resonance integrates to three protons, consistent with formation of the dihydrogen complex, **1-H(Si)(H$_2$)** (eq 5). As with

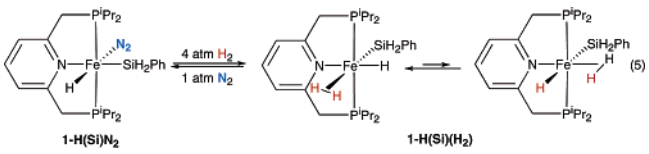

1-H$_2$(H$_2$), the observation of a single peak in the iron-hydride region demonstrates rapid exchange between the Fe−H and

(18) Ricci, J. S.; Koetzle, T. F.; Bautista, M. T.; Hofstede, T. M.; Morris, R. H.; Sawyer, J. F. *J. Am. Chem. Soc.* **1989**, *111*, 8823.
(19) Ho, N. N.; Bau, R.; Mason, S. A. *J. Organomet. Chem.* **2003**, *676*, 85.
(20) Van Der Sluys, L. S.; Eckert, J.; Eisenstein, O.; Hall, J. H.; Huffman, J. C.; Jackson, S. A.; Koetzle, T. F.; Kubas, G. J.; Vergamini, P. J.; Caulton, K. G. *J. Am. Chem. Soc.* **1990**, *112*, 4831.

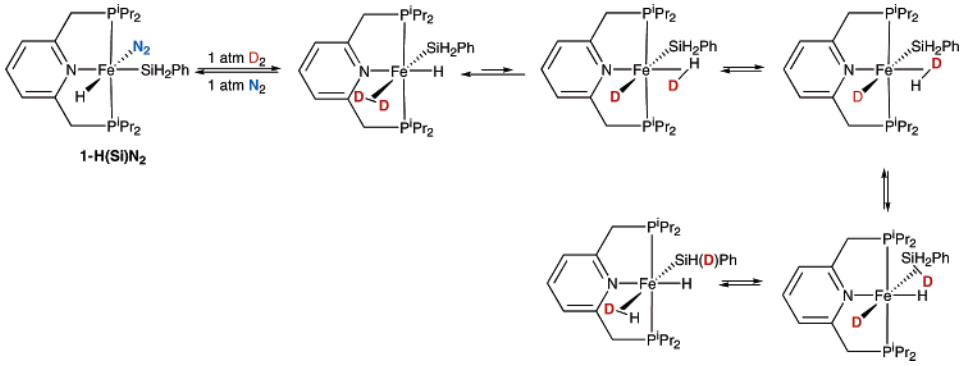

Figure 5. Proposed pathway for isotopic exchange in **1-H(Si)N_2** upon treatment with D_2 gas.

η^2-H_2 ligand. The benzene-d_6 EXSY NMR spectrum (500 ms mixing time) established no exchange between the iron-hydride/dihydrogen ligands and the silicon hydrogens on the NMR time scale. Based on these observations, one of the three possible isomers, the one in which the iron-hydride and the η^2-H_2 are trans, was eliminated.

Observation of both **1-H(Si)N_2** and **1-H(Si)(H_2)** again suggests slow dissociation of N_2 in the substitution of dihydrogen for dinitrogen. Complete conversion to **1-H(Si)(H_2)** was not observed after multiple additions of 4 atm of dihydrogen, demonstrating the affinity of the iron for N_2 relative to H_2. To probe if a silane σ-complex was accessible, **1-H(Si)N_2** was treated with 4 atm of D_2. As expected, the iron-hydride resonance disappeared rapidly with concomitant loss of H−D gas as evidenced by ^{1}H NMR spectroscopy. At slightly longer reaction times, disappearance of the silicon hydride resonances was also observed, establishing the intermediacy of a silane σ-complex (Figure 5). To account for the observation of free H−D, dissociative substitution of D_2 for η^2-H−D occurs, most likely from the isomer where the σ ligand is trans to the silyl, a result of the strong trans effect of silyl ligands.[21] Isotopic exchange with benzene-d_6 was not observed with either **1-H_2(N_2)** or **1-H(Si)N_2**.

The rapid exchange of the hydride ligands in both **1-H_2(H_2)** and **1-H(Si)(H_2)** is intriguing in light of results concerning the structure and dynamics of iron hydride−dihydrogen complexes where these two ligands are cis. The majority of known iron hydride−dihydrogen compounds are cationic bis(diphosphine) compounds where the Fe−H is trans to the η^2-H_2 ligand.[22−25] Other cationic examples where the hydride and η^2-dihydrogen are cis have been reported with tetradentate phosphine chelates[26−29] and are generally prepared by protonation of the neutral iron dihydride precursor. A neutral example, relevant to the compounds reported in this work, is $(Ph_2EtP)_3FeH_2(H_2)$, originally prepared by Aresta and co-workers.[30] Subsequent neutron diffractions studies established an iron(II) dihydrogen−dihydride complex where the η^2-H_2 ligand rapidly exchanges with the iron-hydrides on the NMR time scale even at low temperature.[20] In cases where the hydride and η^2-dihydrogen are cis, the rapid exchange has been rationalized by a phenomenon termed the "cis-effect" rather than by oxidation to iron(IV).[17,20,31,32] The rationale for this effect is an electrostatic attraction between the iron-hydride and the η^2-dihydrogen ligand via a diplole/induced dipole interaction, e.g., $Fe-H^{\delta-}\cdots H^{\delta+}-H^{\delta-}$. Such an interaction is plausible and would account for the rapid exchange observed in both **1-H_2(H_2)** and **1-H(Si)(H_2)**. To our knowledge, such an interaction has not been computed for exchange with silane ligands and oxidative addition to Fe(IV) may be required to account for the slower isotopic exchange into the silyl ligand.

Simple ligand substitution reactions were also studied with both **1-H_2(N_2)** and **1-H(Si)N_2**. Addition of 4 atm of carbon monoxide to **1-H_2(N_2)** induced rapid reductive elimination of H_2 and formation of the dicarbonyl complex, **1-$(CO)_2$** (eq 6). Performing the same experiment with **1-H(Si)N_2** resulted

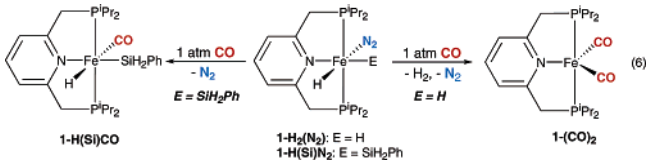

(6)

in substitution of the dinitrogen ligand with carbon monoxide to form **1-H(Si)CO** (eq 6). Extended thermolysis of **1-H(Si)CO** at 95 °C for 1 week under excess CO produced approximately 50% conversion to **1-$(CO)_2$**, establishing the higher barrier for Si−H reductive coupling and dissociation compared to H_2.

The solid-state (KBr) infrared spectrum of **1-H(Si)CO** exhibited a strong carbonyl band centered at 1879 cm^{-1}, a higher frequency than those observed with **1-$(CO)_2$**, consistent with an iron(II) center in the former. A diagnostic iron-

(21) Dioumaev, V. K.; Procopio, L. J.; Caroll, P. J.; Berry, D. H. *J. Am. Chem. Soc.* **2003**, *125*, 8043.
(22) Gilbertson, J. D.; Szymczak, N. K.; Tyler, D. R. *Inorg. Chem.* **2004**, *43*, 3341.
(23) Morris, R. H.; Sawyer, J. F.; Shiralian, M.; Zubkowski, J. D. *J. Am. Chem. Soc.* **1985**, *107*, 5581.
(24) Bautista, M.; Earl, K. A.; Morris, R. H.; Sella, A. *J. Am. Chem. Soc.* **1987**, *109*, 3780.
(25) Helleren, C. A.; Henderson, R. A.; Leigh, G. J. *J. Chem. Soc., Dalton Trans.* **1999**, 1213.
(26) Field, L. D.; Li, H. L.; Messerle, B. A.; Smernik, R. J.; Turner, P. *Dalton Trans.* **2004**, 1418.
(27) Bampos, N.; Field, L. D. *Inorg. Chem.* **1990**, *29*, 587.
(28) Jia, G.; Drouin, S. D.; Jessop, P. G.; Lough, A. J.; Morris, R. H. *Organometallics* **1993**, *12*, 906.
(29) (a) Bianchini, C.; Peruzzini, M.; Polo, A.; Vacca, A.; Zanobini, F. *Gazz. Chim. Ital.* **1991**, *121*, 543. (b) Bianchini, C.; Peruzzini, M.; Zanobini, F. *J. Organomet. Chem.* **1988**, *354*, C19.
(30) Aresta, M.; Giannoccaro, P.; Rossi, M.; Sacco, A. *Inorg. Chim. Acta* **1971**, *5*, 115.

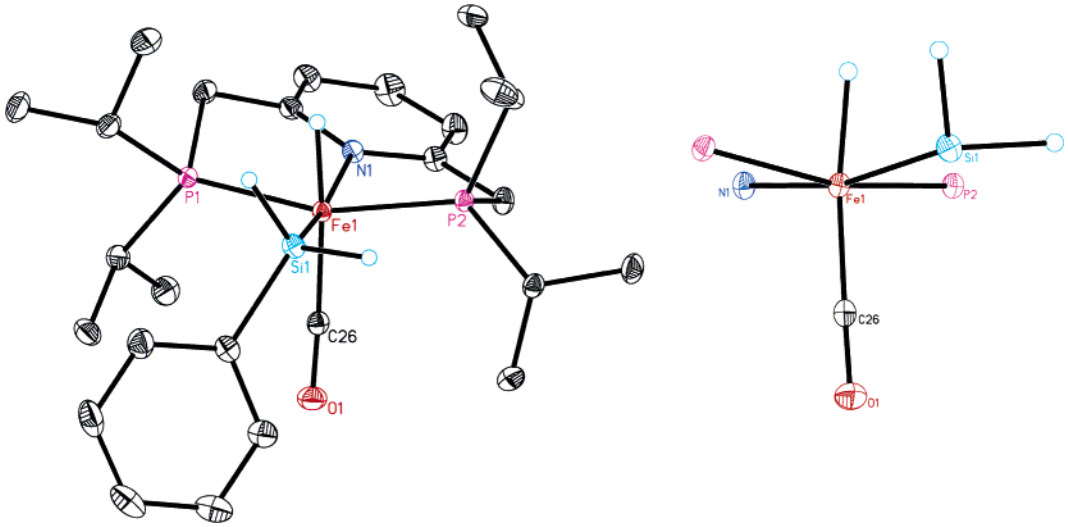

Figure 6. (a) Molecular structure of **1-H(Si)CO** depicted with 30% probability ellipsoids. (b) View of the core of the molecule highlighting the distortion from idealized octahedral coordination. Hydrogen atoms, except for the iron-hydride and silicon hydrogens, omitted for clarity.

hydride resonance was observed at −6.41 ppm by ^{1}H NMR spectroscopy, and a single ^{31}P peak was identified at 103.86 ppm. **1-H(Si)CO** was also characterized by single-crystal X-ray diffraction. A representation of the solid-state structure is presented in Figure 6, and selected metrical parameters are reported in Table 2. A similar distortion from idealized octahedral geometry is observed with **1-H(Si)CO** as was with its dinitrogen congener. The P(1)−Fe(1)−P(2) and N(1)−Fe(1)−Si(1) angles of 160.761(19)° and 167.02(4)° are deviated from linearity as is the H(1M)−Fe(1)−C(26) angle of 166.2(9)°. A slightly more pronounced silicon−iron hydride interaction is evident in the carbonyl compound with a Si(1)−Fe(1)−H(1) angle of 75.9(9)°.

The C(26)−O(1) bond length of 1.1635(19) Å is slightly shorter than the corresponding values of 1.1734(11) Å found in the iron(0) complex, **1-(CO)$_2$**. The distance between the iron-hydride and the silyl ligand of 2.41(2) Å is comparable to the dinitrogen complex, **1-H(Si)N$_2$**, and is outside the sum of the covalent radii. In addition, a short N(1)−C(2) distance of 1.359(2) Å is found in the pyridine ring, indicating that the ligand is not involved in electron-transfer processes with the iron.

Treatment of **1-H(Si)N$_2$** with 1 equiv of PMe_3 produced a similar outcome as carbon monoxide, resulting in substitution of the N_2 by the phosphine (eq 7). Assignment of the

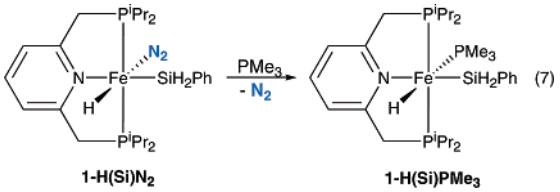

stereochemistry of **1-H(Si)PMe$_3$** was accomplished by two-dimensional NOESY NMR spectroscopy. Cross-peaks were observed between the iron hydride, the Si−H peaks, and the ortho-phenyl of the silyl ligand. Notably, no cross-peaks were observed between the phosphine ligand and the iron hydride, suggesting a trans arrangement. The iron-hydride resonance was observed by ^{1}H NMR spectroscopy in benzene-d_6 as a triplet of doublets centered at −9.97 ppm. Notably, the coupling to the cis phosphines on the ^{iPr}PNP ligand is 67 Hz, larger than the value of 21.0 Hz determined for the coupling to the "trans" PMe_3 ligand. The origin of the unusual magnitudes of the coupling constants is believed to be a result of the distortion from idealized octahedral geometry in analogy to the solid-state structures of **1-H(Si)N$_2$** and **1-H(Si)CO**. In this arrangement, the distortion of the Me_3P−Fe−H bond from linearity reduces the coupling constant.

Because unusual coupling constants were observed with **1-H(Si)PMe$_3$**, the spin−spin coupling in molecules of known stereochemistry was examined. The cis H−Fe−Si coupling constants in **1-H(Si)N$_2$** and **1-H(Si)CO** are similar with values of 28.0 and 25.0 Hz, respectively. A smaller coupling constant of 12.5 Hz was measured for **1-H(Si)PMe$_3$**. The isotopically labeled compound, **1-H(Si)^{13}CO** was prepared in a straightforward manner by treatment of **1-H(Si)N$_2$** with ^{13}CO. The trans H−Fe−^{13}C coupling constant of 10.5 Hz is smaller than the cis P−Fe−^{13}C coupling constant of 14.0 Hz. However, these values must be treated with caution as the coupling to different atoms may not be compared directly and previous work by Whitesides and Maglio has demonstrated that H−M−^{13}C coupling constants are not directly related to stereochemistry.[33]

To gain additional insight about the poor performance of **1-H(Si)N$_2$** in catalytic hydrosilation, reactions with olefins and alkynes were explored. Addition of a large excess (>50 equiv) of 2-butyne to **1-H(Si)N$_2$** resulted in immediate loss of the ^{iPr}PNP ligand, as judged by ^{1}H and ^{31}P NMR spectroscopy (eq 8). Analysis of the organic products by mass

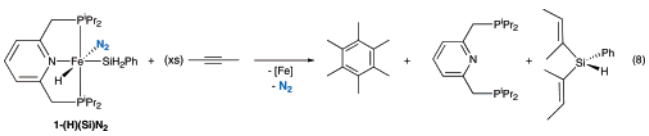

spectrometry and NMR spectroscopy revealed formation of hexamethylbenzene and $(Me(H)C=(Me)C)_2PhSiH$. The iron product(s) of the reaction has not been identified.

Similar experiments were conducted with olefins. Treatment of **1-H(Si)N$_2$** with a large excess (>50 equiv) of 1-hexene or cyclohexene produced no change in the ^{1}H NMR spectrum over the course of days at 23 °C. In contrast, addition of a large excess of ethylene yielded (diethyl)-phenylsilane, Et_2PhSiH, along with a yellow powder that is insoluble in most common organic solvents. While the exact identity of this compound is unknown at this time, degradation experiments establish an iron compound containing ^{iPr}PNP and ethylene-derived ligands. This material is unreactive toward excess olefin and silanes, offering insight into the inability of **1-H(Si)N$_2$** to catalyze olefin hydrosilation.

Concluding Remarks

The studies described herein highlight the ability of saturated bis(phosphino)pyridine ligands to engender more reducing iron centers than aryl-substituted bis(imino)pyridine chelates. In addition to more reduced carbonyl ligands, the pincer-ligated compounds promote oxidative addition of dihydrogen and phenyl silane forming observable ferrous dihydride and silyl hydride compounds. Exposure of these molecules to a dihydrogen atmosphere allowed observation of dihydrogen σ-complexes where the iron-hydride and the η^2-dihydrogen ligands are in rapid exchange in solution. These compounds, unlike the bis(imino)pyridine counterparts, do not engage in redox processes with the iron center and hence are more prone to dissociation.

Experimental Section

General Considerations. All air- and moisture-sensitive manipulations were carried out using standard vacuum line, Schlenk, and cannula techniques or in an MBraun inert atmosphere drybox containing an atmosphere of purified nitrogen. The MBraun drybox was equipped with a cold well designed for freezing samples in liquid nitrogen. Solvents for air- and moisture-sensitive manipulations were initially dried and deoxygenated using literature procedures.[34] Argon and hydrogen gas were purchased from Airgas Incorporated and passed through a column containing manganese oxide supported on vermiculite and 4 Å molecular sieves before admission to the high-vacuum line. Benzene-d_6 was purchased from Cambridge Isotope Laboratories and distilled from 4 Å molecular sieves under an atmosphere of argon and stored over 4 Å molecular sieves and sodium metal. Carbon monoxide was purchased from Aldrich and passed through a liquid nitrogen trap before use. Ethylene was purchased from Aldrich, passed through a liquid-nitrogen-cooled trap, and stored over a slurry of activated MAO in toluene before use. Sodium triethylborohydride was obtained from Aldrich in a 1.0 M solution in toluene and used as received. Phenylsilane, 1-hexene, cyclohexene, trimethylphosphine, and 2-butyne were purchased from Acros or Aldrich and dried over activated molecular sieves before use. The iron(II) dihalide complexes, **1-Cl$_2$** and **1-Br$_2$**, were prepared as described previously.[11]

^{1}H, ^{13}C, and ^{31}P NMR spectra were recorded at 399.780 or 500.62, 101.535 or 125.893, and 161.833 or 202.648 MHz, respectively, using Inova 400 and 500 spectrometers. ^{1}H and $\{^1H\}^{13}$C NMR chemical shifts are reported in ppm downfield from tetramethylsilane using ^{1}H (residual) chemical shifts of the solvent as a secondary standard. $\{^1H\}^{31}$P NMR and ^{31}P chemical shifts are reported downfield from H_3PO_4 and referenced to an external 85% H_3PO_4 solution. Single crystals suitable for X-ray diffraction were coated with polyisobutylene oil in a drybox and were quickly transferred to the goniometer head of a Bruker ×8 APEX2 system equipped with a molybdenum X-ray tube (λ = 0.71073 A). Preliminary data revealed the crystal system. A hemisphere routine was used for data collection and determination of lattice constants. The space group was identified and the data were processed using the Bruker SAINT program and corrected for absorption using SADABS. The structures were solved using direct methods (SHELXS) completed by subsequent Fourier synthesis and refined by full-matrix least-squares procedures. Elemental analyses were performed at Robertson Microlit Laboratories, Inc. in Madison, NJ.

Preparation of [(2,6-^{i}Pr$_2$PCH$_2$)$_2$C$_5$H$_3$N]Fe(CO)$_2$ (1-(CO)$_2$). A thick-walled reaction vessel was charged with 0.500 g (0.901 mmol) of **1-Br$_2$** and ~50 mL of pentane. A 0.5% sodium amalgam prepared from 0.104 g (4.51 mmol) of sodium metal and 21.7 g (901 mmol) of mercury was added to the vessel, and the resulting slurry was frozen to liquid nitrogen temperature. On a high-vacuum line, the vessel was evacuated and 1 atm of carbon monoxide was added at −196 °C. The resulting reaction mixture was warmed to ambient temperature and stirred for 48 h, over which time a royal blue solution formed. The carbon monoxide was then removed from the vessel, and the solution decanted away from the amalgam and filtered through Celite. The filtrate was collected and the solvent was removed in vacuo to yield 0.394 g (97%) of a red solid identified as **1-(CO)$_2$**. Analysis for $C_{21}H_{35}FeNO_2P_2$: Calcd C, 55.89; H, 7.82; N 3.10. Found: C, 55.36; H, 7.65; N, 2.77. ^{1}H NMR (benzene-d_6): δ = 1.17 (pseudo q, J_{HH} = 6.5 Hz, 12H, CH(C*H*$_3$)$_2$), 1.23 (pseudo q, J_{HH} = 6.5 Hz, 12H, CH(C*H*$_3$)$_2$), 2.16 (m, 4H, C*H*(CH$_3$)$_2$), 2.79 (m, 4H, PC*H*$_2$), 6.34 (d, J_{HH} = 7.0 Hz, 2H, *3,5 py-H*), 6.55 (t, J_{HH} = 7.0 Hz, 1H, *4 py-H*). ^{13}C NMR (THF-d_8): δ = 18.72 (s, CH(*C*H$_3$)$_2$), 18.74 (s, CH(*C*H$_3$)$_2$), 28.80 (t, J_{PC} = 10.5 Hz, *C*H(CH$_3$)$_2$), 41.15 (t, J_{PC} = 8.5 Hz, P*C*H$_2$), 119.28 (t, J_{PC} = 5.0 Hz, *3,5* py-C), 131.15 (s, *4 py-C*), 162.49 (t, J_{PC} = 6.0 Hz, *2,6 py-C*), 223.07 (t, J_{PC} = 27.0 Hz, Fe-*C*O). $\{^1H\}^{31}$P NMR (THF-d_8): δ = 109.59 (s). IR (KBr): ν_{CO} = 1794, 1842 cm^{-1}.

Preparation of [(2,6-^{i}Pr$_2$PCH$_2$)$_2$C$_5$H$_3$N]FeH$_2$(N$_2$) (1-H$_2$(N$_2$)). A 100 mL round-bottomed flask was charged with 1.00 g (2.16 mmol) of **1-Cl$_2$** and ~50 mL of diethyl ether. The resulting slurry was frozen in a liquid-nitrogen-cooled cold well. To the thawing slurry, 0.543 g (4.32 mmol) of $NaBEt_3H$ (from a 1.0 M solution in toluene) was added dropwise to the flask. Immediately upon addition, a dark purple solution formed. The reaction mixture was stirred for 1 h and then filtered through Celite. The filtrate was collected and the solvent removed in vacuo. The resulting residue was washed three times with small portions of diethyl ether to yield 0.333 g (36%) of a red-orange solid identified as **1-H$_2$(N$_2$)**. Analysis for $C_{19}H_{37}FeN_3P_2$: Calcd C, 53.66; H, 8.77; N 9.88. Found: C, 53.95; H, 8.46; N, 10.18. ^{1}H NMR (benzene-d_6): δ = −17.65 (td, J_{HH} = 21.5 Hz, J_{PH} = 52.0 Hz, 1H, Fe-*H*), −12.54 (td, J_{HH} = 21.5 Hz, J_{PH} = 60.5 Hz, 1H, Fe-*H*), 0.91 (pseudo q, J_{HH} = 7.0 Hz, 6H, CH(C*H*$_3$)$_2$), 1.21 (pseudo q, J_{HH} = 7.0 Hz, 6H, CH(C*H*$_3$)$_2$), 1.31 (m, 12H, CH(C*H*$_3$)$_2$), 1.94 (m, 2H, C*H*(CH$_3$)$_2$), 2.29 (m, 2H, C*H*(CH$_3$)$_2$), 2.90 (m, 2H, PC*H*$_2$), 3.07 (m, 2H, PC*H*$_2$), 6.48 (d, J_{HH} = 7.0 Hz, 2H, *3,5 py-H*), 6.63 (t, J_{HH} = 7.0 Hz, 1H, *4 py-H*). ^{13}C NMR (benzene-d_6): δ = 19.06 (s, CH(*C*H$_3$)$_2$), 19.22 (s, CH(*C*H$_3$)$_2$), 20.04 (s, CH(*C*H$_3$)$_2$), 20.15 (s, CH(*C*H$_3$)$_2$), 26.74 (t, J_{PC} = 14.0 Hz, *C*H(CH$_3$)$_2$), 27.77 (t, J_{PC} = 6.5 Hz, *C*H(CH$_3$)$_2$), 41.70 (t, J_{PC}

(31) Bianchini, C.; Masi, D.; Peruzzini, M.; Casarin, M.; Maccato, C.; Rizzi, G. A. *Inorg. Chem.* **1997**, *36*, 1061.
(32) (a) Jackson, S. A.; Eisenstein, O. *Inorg. Chem.* **1990**, *29*, 3410. (b) Riehl, J.-F.; Pélissier, M.; Eisenstein, O. *Inorg. Chem.* **1992**, *31*, 3344.
(33) Whitesides, G. M.; Maglio, G. *J. Am. Chem.* **1969**, *91*, 4980.
(34) Pangborn, A. B.; Giardello, M. A.; Grubbs, R. H.; Rosen, R. K.; Timmers, F. J. *Organometallics* **1996**, *15*, 1518.

= 5.5 Hz, P*C*H$_2$), 118.07 (t, J_{PC} = 4.5 Hz, *3,5 py-C*), 130.57 (s, *4 py-C*), 164.47 (t, J_{PC} = 6.0 Hz, *2,6 py-C*). {^{1}H}^{31}P NMR (benzene-d_6): δ = 108.28 (s). ^{31}P NMR (benzene-d_6): δ = 108.28 (t, J_{PH} = 52.0 Hz). IR (KBr): ν_{NN} = 2016 cm^{-1}.

Preparation of [(2,6-^{i}Pr$_2$PCH$_2$)$_2$C$_5$H$_3$N]FeH(SiH$_2$Ph)N$_2$ (1-H(Si)N$_2$). A 100 mL round-bottomed flask was charged with 0.635 g (1.36 mmol) of **1-Cl$_2$**, 0.147 g (1.36 mmol) of phenylsilane and ~60 mL of diethyl ether. After the solution was chilled in a liquid-nitrogen-cooled cold well for 15 min, 0.332 g (2.73 mmol) of NaBEt$_3$H (from a 1.0 M solution in toluene) was slowly added dropwise while stirring. After 3 h, the orange reaction mixture was filtered through Celite and the solvent was removed in vacuo. Recrystallization of the resulting residue from pentane at −35 °C yielded 0.588 g (81%) of an orange solid identified as **1-H(Si)N$_2$**. Analysis for $C_{25}H_{43}FeN_3P_2Si$: Calcd C, 56.49; H, 8.15; N 7.91. Found: C, 56.53; H, 8.37; N, 7.64. ^{1}H NMR (benzene-d_6): δ = −13.12 (t, J_{PH} = 57.5 Hz, 1H, Fe-*H*), 0.64 (pseudo q, J_{HH} = 7.0 Hz, 6H, CH(C*H*$_3$)$_2$), 0.94 (pseudo q, J_{HH} = 7.0 Hz, 6H, CH(C*H*$_3$)$_2$), 1.26 (m, 12H, CH(C*H*$_3$)$_2$), 2.16 (m, 2H, C*H*(CH$_3$)$_2$), 2.39 (m, 2H, C*H*(CH$_3$)$_2$), 2.71 (m, 2H, PC*H*$_2$), 2.97 (m, 2H, PC*H*$_2$), 4.94 (t, J_{PH} = 5.5 Hz, 1H, Si*H*$_2$), 4.95 (t, J_{PH} = 5.5 Hz, 1H, Si*H*$_2$), 6.48 (d, J_{HH} = 7.5 Hz, 2H, *3,5 py-H*), 6.68 (t, J_{HH} = 7.5 Hz, 1H, *4 py-H*), 7.23 (m, 1H, *4 phenyl-H*), 7.35 (m, 2H, *3,5 phenyl-H*), 8.15 (m, 2H, *2,6 phenyl-H*). ^{13}C NMR (benzene-d_6): δ = 17.87 (s, CH(*C*H$_3$)$_2$), 18.32 (s, CH(*C*H$_3$)$_2$), 18.92 (s, CH(*C*H$_3$)$_2$), 19.20 (s, CH(*C*H$_3$)$_2$), 25.47 (t, J_{PC} = 14.0 Hz, *C*H(CH$_3$)$_2$), 27.48 (t, J_{PC} = 7.5 Hz, *C*H(CH$_3$)$_2$), 38.47 (t, J_{PC} = 5.0 Hz, P*C*H$_2$), 118.84 (t, J_{PC} = 4.0 Hz, *3,5 py-C*), 126.79 (s, *4 phenyl-C*), 127.57 (s, *3,5 phenyl-C*), 132.78 (s, *4 py-C*), 136.29 (s, *2,6 phenyl-C*), 149.48 (s, *1 phenyl-C*), 163.33 (t, J_{PC} = 5.5 Hz, *2,6 py-C*). {^{1}H}^{31}P NMR (benzene-d_6): δ = 96.85 (s). IR (KBr): ν_{NN} = 2032 cm^{-1}.

Preparation of [(2,6-^{i}Pr$_2$PCH$_2$)$_2$C$_5$H$_3$N]FeH(SiH$_2$Ph)CO (1-H(Si)CO). A thick-walled reaction vessel was charged with 0.200 g (0.376 mmol) of **1-H(Si)N$_2$** and ~50 mL of pentane. The vessel was submerged in liquid nitrogen and evacuated. At this temperature, 1 atm of carbon monoxide was added. The resulting reaction mixture was warmed to ambient temperature and stirred for 3 h, forming a green solution. After 2 days of stirring, the vessel was submerged in liquid nitrogen and evacuated. The solvent was removed in vacuo and the resulting residue recrystallized from diethyl ether at −35 °C to yield 0.117 g (56%) of an olive green solid identified as **1-H(Si)CO**. Analysis for $C_{26}H_{43}FeNOP_2Si$: Calcd C, 58.75; H, 8.15; N, 2.64. Found: C, 58.50; H, 8.03; N, 2.76. ^{1}H NMR (benzene-d_6): δ = −6.41 (t, J_{PH} = 55.0 Hz, 1H, Fe-*H*), 0.67 (pseudo q, J_{HH} = 7.0 Hz, 6H, CH(C*H*$_3$)$_2$), 0.96 (pseudo q, J_{HH} = 7.0 Hz, 6H, CH(C*H*$_3$)$_2$), 1.26 (pseudo q, J_{HH} = 7.0 Hz, 6H, CH(C*H*$_3$)$_2$), 1.35 (pseudo q, J_{HH} = 7.0 Hz, 6H, CH(C*H*$_3$)$_2$), 2.14 (m, 2H, C*H*(CH$_3$)$_2$), 2.24 (m, 2H, C*H*(CH$_3$)$_2$), 2.74 (m, 2H, PC*H*$_2$), 2.88 (m, 2H, PC*H*$_2$), 4.94 (t, J_{PH} = 5.0 Hz, 1H, Si*H*$_2$), 4.95 (t, J_{PH} = 5.0 Hz, 1H, Si*H*$_2$), 6.40 (d, J_{HH} = 7.5 Hz, 2H, *3,5 py-H*), 6.66 (t, J_{HH} = 7.5 Hz, 1H, *4 py-H*), 7.22 (t, J_{HH} = 7.5 Hz, 1H, *4 phenyl-H*), 7.33 (t, J_{HH} = 7.5 Hz, 2H, *3,5 phenyl-H*), 8.21 (d, J_{HH} = 7.5 Hz, 2H, *2,6 phenyl-H*). ^{13}C NMR (benzene-d_6): δ = 17.63 (s, CH(*C*H$_3$)$_2$), 18.03 (s, CH(*C*H$_3$)$_2$), 18.61 (s, CH(*C*H$_3$)$_2$), 19.18 (s, CH(*C*H$_3$)$_2$), 25.39 (t, J_{PC} = 13.0 Hz, *C*H(CH$_3$)$_2$), 27.00 (t, J_{PC} = 10.0 Hz, *C*H(CH$_3$)$_2$), 39.50 (t, J_{PC} = 6.5 Hz, P*C*H$_2$), 118.69 (t, J_{PC} = 4.5 Hz, *3,5 py-C*), 126.13 (s, *4 phenyl-C*), 127.52 (s, *3,5 phenyl-C*), 133.17 (s, *4 py-C*), 136.38 (s, *2,6 phenyl-C*), 149.37 (s, *1 phenyl-C*), 162.86 (t, J_{PC} = 5.5 Hz, *2,6* py-C), 220.89 (t. J_{PC} = 14.0 Hz, Fe-*C*O). {^{1}H}^{31}P NMR (benzene-d_6): δ = 103.86 (s). IR (KBr): ν_{CO} = 1879 cm^{-1}.

Preparation of [(2,6-^{i}Pr$_2$PCH$_2$)$_2$C$_5$H$_3$N]FeH(SiH$_2$Ph)(P(CH$_3$)$_3$) (1-H(Si)PMe$_3$). This compound was prepared in a manner similar to that described for **1-H(Si)CO** using 0.040 g (0.075 mmol) of **1-H(Si)N$_2$** and 1 equiv of PMe$_3$ yielding 0.035 g (80%) of a dark purple solid identified as **1-H(Si)PMe$_3$**. Analysis for $C_{28}H_{52}FeNOP_3Si$: Calcd C, 58.03; H, 9.04; N, 2.42. Found: C, 57.87; H, 9.29; N, 2.31. ^{1}H NMR (benzene-d_6): δ = −9.97 (td, J_{PH} (PMe$_3$) = 21.0 Hz, J_{PH} (P^{i}Pr$_2$) = 67.0 Hz, 1H, Fe-*H*), 0.97 (pseudo q, J_{HH} = 6.5 Hz, 6H, CH(C*H*$_3$)$_2$), 1.07 (pseudo q, J_{HH} = 6.5 Hz, 6H, CH(C*H*$_3$)$_2$), 1.10 (d, J_{PH} = 5.5 Hz, 9H, P(C*H*$_3$)$_3$), 1.29 (pseudo q, J_{HH} = 6.5 Hz, 6H, CH(C*H*$_3$)$_2$), 1.39 (pseudo q, J_{HH} = 6.5 Hz, 6H, CH(C*H*$_3$)$_2$), 2.16 (m, 2H, C*H*(CH$_3$)$_2$), 2.43 (m, 2H, C*H*(CH$_3$)$_2$), 2.60 (m, 2H, PC*H*$_2$), 3.03 (m, 2H, PC*H*$_2$) 4.94 (q, J_{PH} = 7.0 Hz, 1H, Si*H*$_2$), 4.95 (q, J_{PH} = 7.0 Hz, 1H, Si*H*$_2$), 6.41 (d, J_{HH} = 7.5 Hz, 2H, *3,5 py-H*), 6.53 (t, J_{HH} = 7.5 Hz, 1H, *4 py-H*), 7.21 (t, J_{HH} = 7.5 Hz, 1H, *4 phenyl-H*), 7.53 (t, J_{HH} = 7.5 Hz, 2H, *3,5 phenyl-H*), 8.32 (d, J_{HH} = 7.5 Hz, 2H, *2,6 phenyl-H*). ^{13}C NMR (benzene-d_6): δ = 19.89 (s, CH(*C*H$_3$)$_2$), 20.11 (s, CH(*C*H$_3$)$_2$), 20.63 (s, CH(*C*H$_3$)$_2$), 20.90 (s, CH(*C*H$_3$)$_2$), 22.15 (d, J_{PC} = 17.0 Hz, P(*C*H$_3$)$_3$), 28.94 (m, *C*H(CH$_3$)$_2$), 32.17 (m, *C*H(CH$_3$)$_2$), 44.26 (t, J_{PC} = 3.0 Hz, P*C*H$_2$), 117.45 (t, J_{PC} = 5.0 Hz, *3,5 py-C*), 126.48 (s, *4 phenyl-C*), 127.06 (s, *3,5 phenyl-C*), 128.68 (s, *4 py-C*), 137.66 (s, *2,6 phenyl-C*), 150.78 (m, *1 phenyl-C*), 164.13 (t, J_{PC} = 5.5 Hz, *2,6 py-C*). {^{1}H}^{31}P NMR (benzene-d_6): δ = 9.83 (t, J_{PP} = 18.0 Hz, *P*Me$_3$), 86.49 (d, J_{PP} = 18.0 Hz, *P*^{i}Pr$_2$). {C*H*}^{31}P NMR (benzene-d_6): δ = 9.83 (pseudo q, J_{PP} = 18.0 Hz, J_{PH} = 21.0 Hz, *P*Me$_3$), 86.49 (dd, J_{PP} = 18.0 Hz, J_{PH} = 67.0 Hz, *P*^{i}Pr$_2$).

Observation of [(2,6-^{i}Pr$_2$PCH$_2$)$_2$C$_5$H$_3$N]FeH(SiH$_2$Ph)(H$_2$) (1-H(Si)(H$_2$)). A J. Young tube was charged with 0.010 g (0.02 mmol) of **1-H(Si)N$_2$** and ~0.5 mL of benzene-d_6. The tube was submerged in liquid nitrogen and evacuated on a high-vacuum line. At this temperature, 1 atm of H_2 was admitted and the tube sealed, thawed, and shaken. Monitoring the reaction by multinuclear NMR spectroscopy established growth of **1-H(Si)(H$_2$)** over the course of hours at 23 °C. ^{1}H NMR (benzene-d_6): δ = −9.37 (br s, 3H, Fe-*H*), 0.94 (pseudo q, J_{HH} = 7.0 Hz, 12H, CH(C*H*$_3$)$_2$), 1.14 (pseudo q, J_{HH} = 7.0 Hz, 12H, CH(C*H*$_3$)$_2$), 2.04 (m, 4H, C*H*(CH$_3$)$_2$), 2.84 (m, 4H, PC*H*$_2$), 5.54 (m, 2H, Si*H*$_2$), 6.45 (d, J_{HH} = 8.0 Hz, 2H, *3,5 py-H*), 6.68 (t, J_{HH} = 8.0 Hz, 1H, *4 py-H*), 7.21 (t, J_{HH} = 7.5 Hz, 1H, *4 phenyl-H*), 7.33 (t, J_{HH} = 7.5 Hz, 2H, *3,5 phenyl-H*), 8.23 (d, J_{HH} = 7.5 Hz, 2H, *2,6 phenyl-H*). {^{1}H}^{31}P NMR (benzene-d_6): δ = 108.36 (s).

Acknowledgment. We thank the David and Lucile Packard Foundation for financial support. P.J.C. is a Cottrell Scholar sponsored by the Research Corporation and a Camille Dreyfus Teacher−Scholar. R.J.T. also thanks Cornell University for partial support through a graduate fellowship.

Supporting Information Available: Crystallographic data for **1-(CO)$_2$**, **1-H(Si)N$_2$**, and **1-H(Si)CO** as cif files and a sample ^{1}H NMR spectrum for **1-(CO)$_2$**. This material is available free of charge via the Internet at http://pubs.acs.org.

IC0608647